Nanoscale Res Lett (2010) 5:1535–1539
DOI 10.1007/s11671-010-9673-3

NANO EXPRESS

Fabrication of Coaxial $Si_{1-x}Ge_x$ Heterostructure Nanowires by O_2 Flow-Induced Bifurcate Reactions

Ilsoo Kim · Ki-Young Lee · Ungkil Kim · Yong-Hee Park · Tae-Eon Park · Heon-Jin Choi

Received: 21 April 2010 / Accepted: 7 June 2010 / Published online: 17 June 2010
© The Author(s) 2010. This article is published with open access at Springerlink.com

Abstract We report on bifurcate reactions on the surface of well-aligned $Si_{1-x}Ge_x$ nanowires that enable fabrication of two different coaxial heterostructure nanowires. The $Si_{1-x}Ge_x$ nanowires were grown in a chemical vapor transport process using $SiCl_4$ gas and Ge powder as a source. After the growth of nanowires, $SiCl_4$ flow was terminated while O_2 gas flow was introduced under vacuum. On the surface of nanowires was deposited Ge by the vapor from the Ge powder or oxidized into SiO_2 by the O_2 gas. The transition from deposition to oxidation occurred abruptly at 2 torr of O_2 pressure without any intermediate region and enables selectively fabricated Ge/$Si_{1-x}Ge_x$ or SiO_2/$Si_{1-x}Ge_x$ coaxial heterostructure nanowires. The rate of deposition and oxidation was dominated by interfacial reaction and diffusion of oxygen through the oxide layer, respectively.

Keywords $Si_{1-x}Ge_x$ nanowires · Coaxial heterostructure · Bifurcate reactions · Interfacial reaction · Diffusion-controlled reaction · Self-limiting oxidation · Kinetics of gas diffusion

Introduction

Heterostructures in semiconductors enable diverse functions in many planar electronic devices [1]. Meanwhile, semiconductor nanowires are unique building blocks of electronics on a nanometer scale. Akin to planar devices, heterostructures in the nanowires should enable diverse functions that are promising for high-performance nanowire devices [2–4]. Indeed, recent studies of heterostructure semiconductor nanowires for electronics, such as diodes [3], field-effect transistors (FETs) [5], sensors [6], and the solar cell [7], have demonstrated the higher performances that are ascribed to heterostructures.

Fabrication of heterostructure nanowires have been mostly carried out by consecutive chemical vapor deposition, which supplies precursors one by one in the order of layer stacking sequences [8, 9]. Limited studies also showed formation of heterostructure nanowires through a self-organization mode in a one-step process [10, 11]. In this study, we report about an approach on the fabrication of coaxial heterostructure $Si_{1-x}Ge_x$ nanowires, which are promising building blocks for high-performance nanoelectronic devices. Our approach is based on the O_2 gas flow-induced bifurcate Ge deposition or oxidation reaction of $Si_{1-x}Ge_x$ nanowires. It enables selectively prepared Ge/$Si_{1-x}Ge_x$ or SiO_2/$Si_{1-x}Ge_x$ coaxial heterostructure nanowires by the kinetics of gas flow.

Experimental Procedure

Figure 1 shows a schematic of our procedure. Compositionally controlled $Si_{1-x}Ge_x$ nanowires were synthesized on an Au catalyst deposited Si (1 1 1) substrates at 900–1,000°C in a chemical vapor transport system [12, 13]. Germanium (Ge, Alfa Aesar, 99.9999%) powder and Si tetrachloride ($SiCl_4$, Aldrich, 99.998%) gas were used as source materials for the synthesis of the nanowires [14]. Ge powder and Si substrates placed in inner quartz tube at a distance of 1 inch were inserted into the center of outer quartz tube. The $SiCl_4$ precursor through a H_2 bubbler

I. Kim · K.-Y. Lee · U. Kim · Y.-H. Park ·
T.-E. Park · H.-J. Choi (✉)
Department of Materials Science and Engineering,
Yonsei University, Seoul 120-749, Korea
e-mail: hjc@yonsei.ac.kr

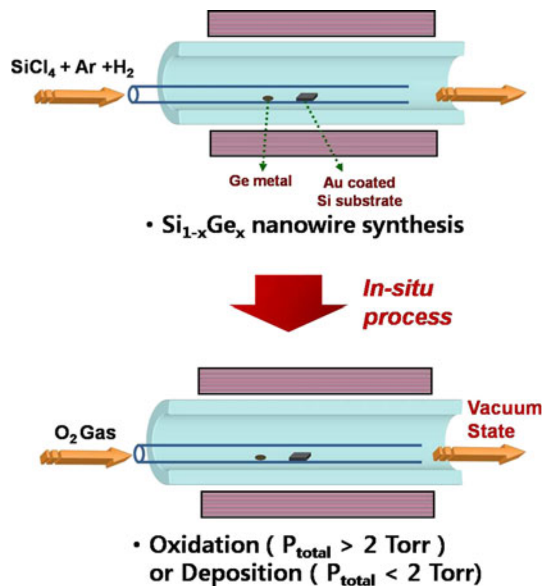

Fig. 1 Schematic of the $Si_{1-x}Ge_x$ heterostructure nanowires synthesized procedure. After the growth of $Si_{1-x}Ge_x$ nanowires, the flow of $SiCl_4$ was terminated and then a flow of O_2 was introduced under vacuum maintained by mechanical pump

system was introduced into the system at a flow rate of 20 sccm. H_2 (100 sccm) and Ar (100 sccm) were used as ambiance gases for the synthesis. After the growth of $Si_{1-x}Ge_x$ nanowires for 30 min, the flow of $SiCl_4$ was terminated and then a flow of O_2 was introduced at 900°C under vacuum maintained by mechanical pump. The flow rate of O_2 was controlled from 50 to 300 sccm for bifurcate reactions.

We observed as-grown $Si_{1-x}Ge_x$ nanowires and modulated coaxial heterostructure nanowires by a scanning electron microscope (SEM) and a high-resolution transmission electron microscopy (HRTEM). High-resolution X-ray diffraction (HR-XRD) measurements were carried out at 3C2 and 11A1 beam line of the Pohang Accelerator Laboratory (PLS).

Results and Discussion

As shown in Fig. 2, the $Si_{1-x}Ge_x$ nanowires for $x = 0.05$, 0.15, and 0.3 were grown and well-aligned on the substrate whose diameter ranged from 50 to 300 nm. The density of nanowires was approximately $10^8/cm^2$. The composition of the $Si_{1-x}Ge_x$ nanowires could be controlled by the substrate distance from the Ge powder [14]. Among them, $Si_{0.85}Ge_{0.15}$ nanowires, which showed better electrical transport properties than other compositions, were investigated for the fabrication of coaxial heterostructures. HRTEM images showed the single crystalline nature with a thin layer of native oxides. The energy-dispersive

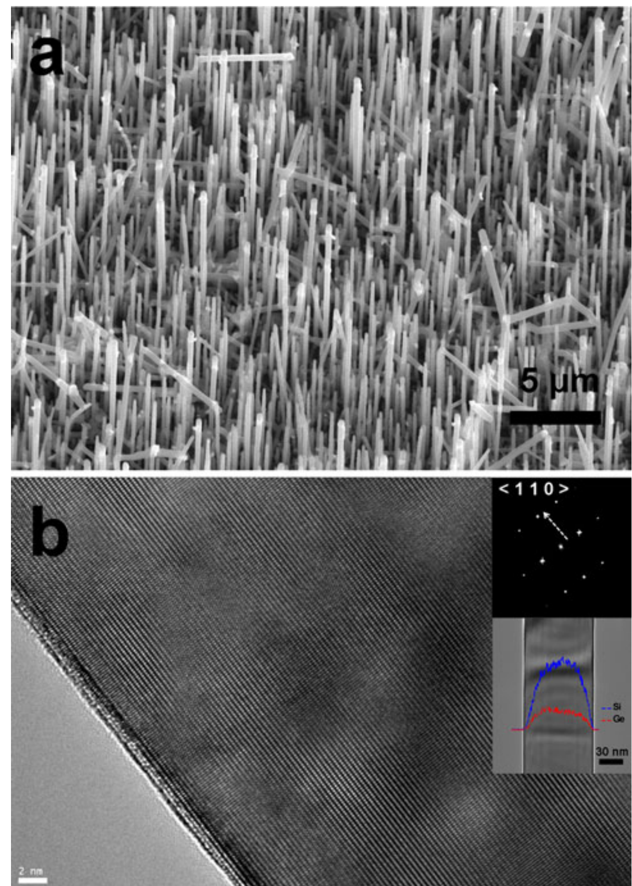

Fig. 2 **a** SEM image of $Si_{1-x}Ge_x$ nanowires with diameter ranged from 50 to 300 nm. **b** TEM image of individual single crystal $Si_{1-x}Ge_x$ nanowires with a thin layer of native oxides. *Upper inset* is SAED pattern image that shows the nanowire is single crystal and a growth direction is <1 1 0>. *Below inset* is EDS profile in the radial direction of the nanowire

spectroscopy (EDS) analysis profile in the radial direction of the nanowire did not show any evidence of phase inhomogeneity; that is, it showed no Ge segregation within the nanowire, as often found in thin film chemical vapor depositions [15, 16].

After the growth of $Si_{1-x}Ge_x$ nanowires, $SiCl_4$ flow was terminated and O_2 gas was introduced under vacuum. Under these conditions, Ge vapor from the Ge source together with O_2 gas were introduced to the substrate where the nanowires were vertically grown. Our systematic studies showed that Ge/$Si_{1-x}Ge_x$ coaxial heterostructure nanowires were the result of the deposition of Ge under the low flow rate of O_2 (i.e., <100 sccm that maintains the total pressure of <2 torr) while SiO_2/$Si_{1-x}Ge_x$ coaxial heterostructure nanowires resulted from the oxidation of $Si_{1-x}Ge_x$ nanowires under the high flow rate (i.e., >100 sccm that maintains the total pressure of >2 torr).

Figure 3 shows the Ge/$Si_{1-x}Ge_x$ coaxial heterostructure nanowires. The synchrotron XRD patterns were indexed to

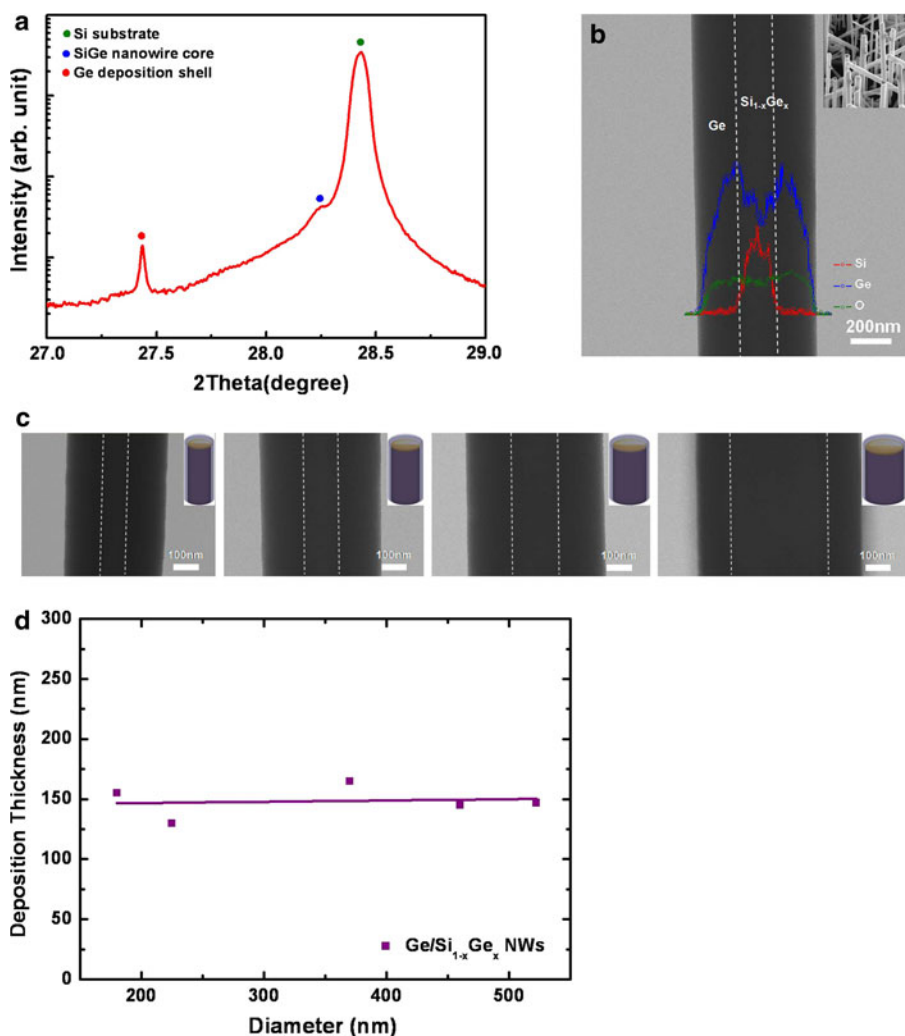

Fig. 3 **a** The synchrotron XRD pattern of Ge/$Si_{1-x}Ge_x$ coaxial heterostructure nanowires. **b** TEM image and EDS profile in the radial direction of Ge/$Si_{1-x}Ge_x$ coaxial heterostructure nanowires. *Inset* is SEM image of the heterostructure nanowires. **c** TEM images measuring the thickness of core and shell as a function of time. *Inset* is schematic of the deposition procedure. **d** Plot of the thickness of Ge shell versus the diameter of $Si_{1-x}Ge_x$ core nanowires

a diamond structure on the $Si_{1-x}Ge_x$ core and Ge deposited on the surface as a shell. The EDS profile in the radial direction of the nanowire clearly shows the uniform thickness of Ge. We investigated the kinetics of the deposition of Ge for different diameters of nanowires by measuring the thickness of the shell as a function of time. As shown in Fig. 3c, the rate of Ge deposition is constant with time. It indicates that Ge deposition on $Si_{1-x}Ge_x$ nanowires was dominated by an interfacial reaction, i.e., the deposition of Ge on the surfaces. It also showed that the rate of deposition was not dependent on the diameter of nanowires.

Figure 4 shows SiO_x/$Si_{1-x}Ge_x$ coaxial heterostructure nanowires. The synchrotron XRD patterns of the oxidized $Si_{1-x}Ge_x$ nanowires were indexed to a diamond structure. The compositional profiles in the radial directions of the oxidized nanowires showed that the composition of the oxide is primarily SiO_x. It was also observed that the (1 1 1) Bragg peak shifted to lower angles with oxidation time. It is due to preferential oxidation of Si in $Si_{1-x}Ge_x$ nanowires that Ge-rich cores result. It is noted that no evidence of Ge segregation, which had frequently been observed in the oxidation of $Si_{1-x}Ge_x$ thin films, was found [17–19]. It is known that Ge segregation in the $Si_{1-x}Ge_x$ nanowires during oxidation is dependent on the rate of oxidation. In a fast oxidation rate, redistribution of Ge may not be achievable, and segregation results. The oxidation rate in this study is thus believed to be rather slow, and Ge is efficiently redistributed over the nanowires and maintains a homogeneous Ge-rich $Si_{1-x}Ge_x$ alloy composition. The shift of (1 1 1) Bragg peak may also due to the growth stresses associated with the oxidation and the thermal mismatch stresses between the SiO_x/$Si_{1-x}Ge_x$ on cooling to the room temperature. The volume expansion of $Si_{1-x}Ge_x$ during oxidation can induce the lattice expansion near the SiO_x/$Si_{1-x}Ge_x$ interface and shift of the (1 1 1) Bragg peak to lower angles [20]. The lattice expansion can also be induced by a thermal expansion coefficient mismatch between the grown SiO_x sheath and the $Si_{1-x}Ge_x$ core [21]. During the cooling to the room temperature, the significant mismatch in the thermal

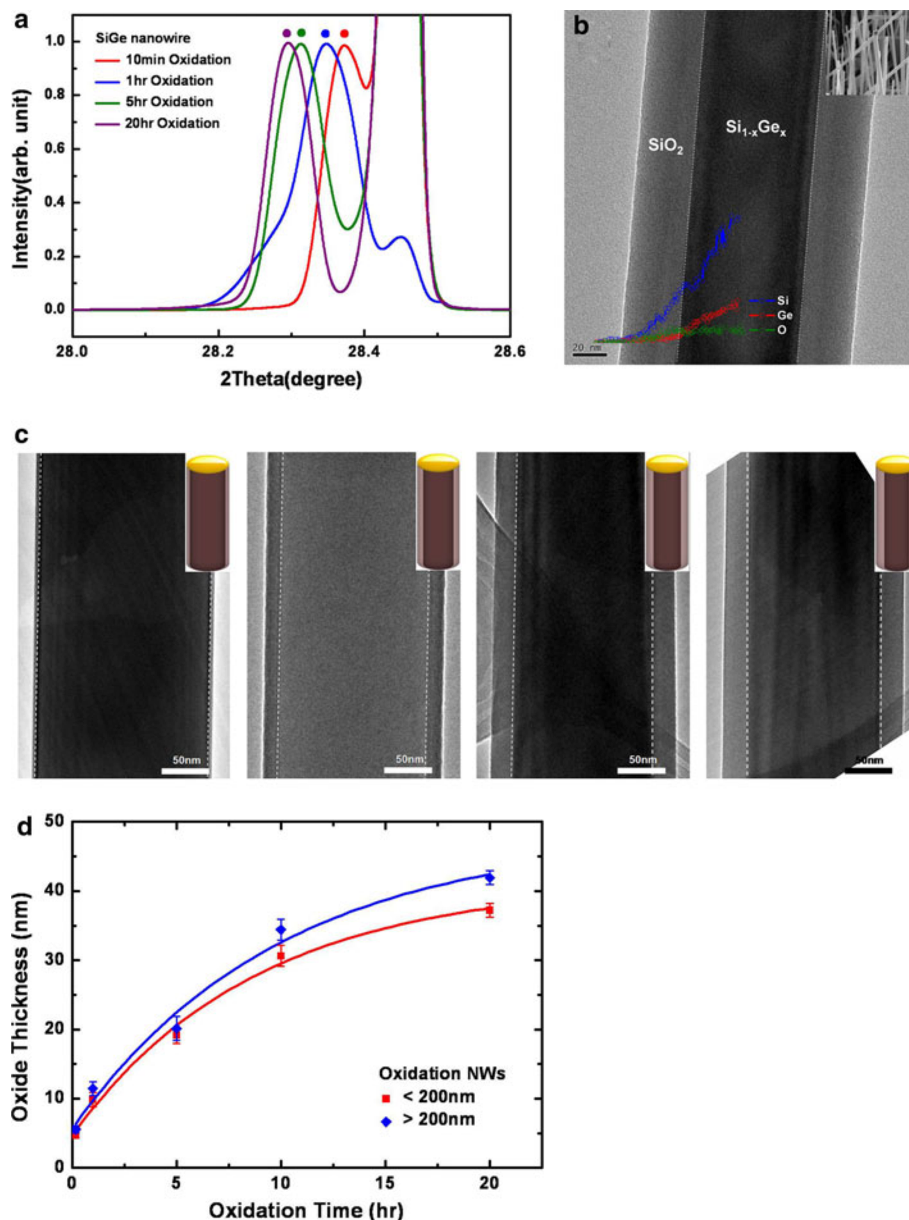

Fig. 4 **a** The synchrotron XRD patterns of SiO_x/$Si_{1-x}Ge_x$ coaxial heterostructure nanowires. **b** TEM image and EDS profile in the radial direction of SiO_x/$Si_{1-x}Ge_x$ coaxial heterostructure nanowires. *Inset* is SEM image of the heterostructure nanowires. **c** TEM images measuring the thickness of core and shell as a function of time. *Inset* is schematic of the oxidation procedure. **d** Plot of the thickness of SiO_x shell versus the oxidation time of $Si_{1-x}Ge_x$ nanowires

expansion coefficients of SiO_x and $Si_{1-x}Ge_x$ ($\sim 5 \times 10^{-7}$ K^{-1} and $\sim 2.9 \times 10^{-6}$ K^{-1} where $x = 0.1$, respectively) can induce tensile stress and lattice expansion in the longitudinal direction of the nanowire and, in turn, shift of the (1 1 1) Bragg peak to lower angles.

The oxidation kinetics of $Si_{1-x}Ge_x$ nanowires was further studied. As shown in Fig. 4, the oxidation thickness follows the typical diffusion-controlled reaction, that is $x_{th} \propto \sqrt{t}$, with self-limiting oxidation [22]. Generally, nanowires show the self-limiting oxidation behavior that can be explained by the evolution of compressive stress normal to the Si/SiO_2 interface [23, 24]. As new oxide grows at the interface, the old oxide expands due to the increase in volume of SiO_2 compared to the core, resulting in a compressive stress normal to the interface that slows the interfacial reaction between the oxidant and Si at the Si/SiO_2 interface. Meanwhile, the magnitude of stresses is inversely proportional to the radius of the curvature of nanowires and thus the oxidation rate depends on the diameters. In fact, the thicker nanowires oxidized faster in this study.

Our results show that $Ge/Si_{1-x}Ge_x$ or $SiO_2/Si_{1-x}Ge_x$ coaxial heterostructure nanowires can be selectively prepared. It is noted that the formation of the shell can be controlled by the flow of O_2 gas. In fact, the reactions were very sensitive to the flow of O_2 pressure and changed abruptly from Ge deposition to oxidation at 2 torr of total pressure without any transition or intermediate region.

Therefore, it could be considered as bifurcate reactions that one of the two reactions is selectively preceded by the initial condition (i.e., O_2 pressure in this study).

The reason for bifurcation could be given as follows. Under our experimental conditions, reactions as follow can occur on the surface of nanowires:

1) Ge(vapor) = Ge(solid) shell
2) O_2(vapor) + Si(solid) in SiGe nanowires = SiO_2(solid) shell

Thermodynamic calculation shows that the equilibrium partial pressure of O_2 for reaction is almost 10^{-24} torr. Therefore, oxidation of $Si_{1-x}Ge_x$ nanowires can be progressed in our experimental conditions. However, nanowires were densely aligned on the substrate where the gas flow is limited. Meanwhile, deposition or oxidation reaction on the surface nanowires requires diffusive penetration of Ge vapor or oxygen from the reactor atmosphere into the dense array of nanowires. It will depend on the mass and partial pressure of vapor components in the atmosphere. Accordingly, the penetration of O_2 into the nanowire array would be rather difficult for Ge due to its light mass [25, 26]. It may be why a Ge layer is deposited under low O_2 pressure of < 2 torr. Meanwhile, at O_2 pressure higher than 2 torr, O_2 can penetrate into the nanowire array and induce oxidation. The bifurcation is thus a result of compete penetration of Ge vapor and O_2 gas into dense nanowire array, and thus can be understood in terms of kinetics of gas diffusion.

Conclusion

In summary, our study demonstrates that bifurcate Ge deposition or oxidation of aligned $Si_{1-x}Ge_x$ nanowires can be achieved by the control of O_2 gas flow kinetics. The process is simple, however, and efficient to fabricate different coaxial heterostructure nanowires with sharp interfaces, as shown in Figs. 2 and 3. It is also noted that there is no transition between the two reactions and thus a high quality shell of Ge or SiO_2 is achieved. Such nanowires would be used as building blocks for the development of high-performance nanowire-based electronics. For example, coaxial heterostructure nanowires would be helpful to improve electrical transporting in nanowire-based transistors [27]. Oxidized nanowires would be helpful in developing advanced nanowire devices such as surround gated transistors [28].

Acknowledgments This research was supported by a grant from the National Research Laboratory program (R0A-2007-000-20075-0) and Nano R&D (Grant No. 2009-0082724) through the National Research Foundation of Korea (NRF) funded by the Ministry of Education, Science & Technology. This work was also supported by Hi Seoul Science (Humanities) Fellowship from Seoul Scholarship Foundation.

Open Access This article is distributed under the terms of the Creative Commons Attribution Noncommercial License which permits any noncommercial use, distribution, and reproduction in any medium, provided the original author(s) and source are credited.

References

1. S.M. Sze, *Physics of Semiconductor Devices*, 2nd edn. (A Wiley-Interscience Publication, New York, 1981)
2. Y. Xia, P. Yang, Y. Sun, Y. Wu, B. Mayers, B. Gates, Y. Yin, F. Kim, H. Yan, Adv. Mater. **15**, 353 (2003)
3. Y. Cui, C.M. Lieber, Science **291**, 851 (2001)
4. C.M. Lieber, Z.L. Wang, MRS Bull. **32**, 99 (2007)
5. Y. Cui, Z. Zhong, D. Wang, W.U. Wang, C.M. Lieber, Nano Lett. **3**, 149 (2003)
6. Y. Cui, Q. Wei, H. Park, C.M. Lieber, Science **293**, 1289 (2001)
7. B. Tian, X. Zheng, T.J. Kempa, Y. Fang, N. Yu, G. Yu, J. Huang, C.M. Lieber, Nature **449**, 885 (2007)
8. L.J. Lauhon, M.S. Gudlksen, D. Wang, C.M. Lieber, Nature **420**, 57 (2002)
9. F. Qian, S. Gradečak, Y. Li, C.Y. Wen, C.M. Lieber, Nano Lett. **5**, 2287 (2005)
10. Y. Xia, Y. Yin, Y. Lu, J. McLellan, Adv. Funct. Mater. **13**, 907 (2003)
11. H.J. Choi, J.C. Johnson, R. He, S.K. Lee, F. Kim, P. Pauzauskie, J. Goldberger, R.J. Saykally, P. Yang, J. Phys. Chem. B **107**, 8721 (2003)
12. R.S. Wagner, W.C. Ellis, Appl. Phys. Lett. **4**, 89 (1964)
13. M.H. Kim, I.S. Kim, Y.H. Park, T.E. Park, J.H. Shin, H.J. Choi, Nanoscale Res. Lett. **5**, 286 (2009)
14. H.K. Seong, E.K. Jeon, M.H. Kim, H. Oh, J.O. Lee, J.J. Kim, H.J. Choi, Nano Lett. **8**, 3656 (2008)
15. S. Fukatsu, K. Fujita, H. Yaguchi, Y. Shiraki, R. Ito, Appl. Phys. Lett. **59**, 2103 (1991)
16. Y. Li, G.G. Hembree, J.A. Venables, Appl. Phys. Lett. **67**, 276 (1995)
17. H.K. Liou, P. Mei, U. Gennser, E.S. Yang, Appl. Phys. Lett. **59**, 1200 (1991)
18. F.K. LeGoues, R. Rosenberg, T. Nguyen, F. Himpsel, B.S. Meyerson, J. Appl. Phys. **65**, 1724 (1989)
19. S. Margalit, A. Bar-Lev, A.B. Kuper, H. Aharoni, A. Neugroschel, J. Cryst. Growth **17**, 288 (1972)
20. E. Hasegawa, A. Ishitani, K. Akimoto, M. Tsukiji, N. Ohta, J. Electrochem. Soc. **142**, 273 (1995)
21. A.E. Pap, K. Kordás, G. Tóth, J. Levoska, A. Uusimäki, J. Vähäkangas, S. Leppävuori, T.F. George, Appl. Phys. Lett. **86**, 041501 (2005)
22. D. Shir, B.Z. Liu, A.M. Mohammad, K.K. Lew, S.E. Mohney, J. Vac. Sci. Technol. B **24**, 1333 (2006)
23. H.I. Liu, D.K. Biegelsen, F.A. Ponce, N.M. Johnson, R.F.W. Pease, Appl. Phys. Lett. **64**, 1383 (1994)
24. H. Cui, C.X. Wang, G.W. Yang, Nano Lett. **8**, 2731 (2008)
25. L.H. Shendalman, J. Chem. Phys. **51**, 2483 (1969)
26. J.F. De La Mora, Phys. Rev. A **25**, 1108 (1982)
27. J. Xiang, W. Lu, Y. Hu, Y. Wu, H. Yan, C.M. Lieber, Nature **441**, 489 (2006)
28. N. Singh et al., IEEE Electron Device Lett. **27**, 383 (2006)